TARGET DETECTION IN ABRUPTLY NON-STATIONARY DOPPLER-SPREAD CLUTTER

Dinesh Ramakrishnan and Jeffrey Krolik

Department of Electrical and Computer Engineering,
Duke University, Durham, NC, 27708-0291, USA

ABSTRACT

This paper addresses the problem of target detection in the presence of Doppler spread clutter which is neither stationary during a coherent integration time (CIT) interval nor across different range bins. This phenomenology occurs, for example, in over-the-horizon skywave HF radar where propagation through moving ionospheric inhomogeneities spreads the surface clutter and the clutter statistics can change quite abruptly during a CIT and across range bins. In these cases, the performance of conventional adaptive techniques suffers from a lack of adequate training data. The method proposed here breaks the full CIT into smaller sub-CIT's which are then extrapolated using low order AR models. The Doppler spread clutter is thus effectively modeled as an abruptly time varying autoregressive (ATVAR) process. Subsequent Doppler processing and coherent combining of the extrapolated sub-CIT's is then performed with improved signal-to-clutter gain since only a small proportion of the sub-CIT's are corrupted by abrupt non-stationary behavior. Moreover, nearly full coherent signal gain against noise is maintained. Initial processing on experimental radar clutter data with injection of a simulated target illustrates that this approach can provide an SCNR improvement of more than 5 dB compared to conventional Doppler processing.

1. INTRODUCTION

This paper addresses the problem of detecting targets in the presence of non-stationary Doppler spread clutter. This is a commonly encountered problem in radar and sonar. Conventional target detection depends on Doppler discrimination of moving targets from surface backscatter. However, in radar applications, radio wave propagation through highly time-varying channels can cause the surface clutter returns to spread significantly in Doppler space, thereby obscuring target signatures. Several approaches have been proposed to mitigate Doppler spread clutter [1, 2]. One approach has been to estimate the time-varying modulation imposed by the channel and then to demodulate the radar return so as to de-spread the clutter [1, 2]. Unfortunately, however, estimates of the temporal modulation are often contaminated by the target, which leads to signal cancellation during the demodulation process. Alternatively, adaptive Doppler filtering methods [2] that use adjacent ranges or azimuths to compute the clutter covariance matrix are prone to failure because of the statistical inhomogeneity of the propagation environment across different ranges and azimuths. More recently, a method which models the clutter as a slowly time-varying AR process has been proposed [4]. Although similar in concept to our approach, the method proposed in [4] has not shown promise with real data. We hypothesize that this is because it is sensitive to rapid transitions in the modulation statistics, which appear to occur frequently in practice.

The approach proposed here is designed to exploit the short-time stationarity of temporal modulation imposed on the surface backscatter, with accommodation for a few rapid transitions. Time-varying autoregressive modeling of clutter return with abrupt transitions is used to design the adaptive Doppler processor in Sections 2 and 3. Receiver operating characteristics (ROC) presented in Section 4 using a target injected into real radar clutter data suggests that the proposed method provides a significant improvement in detection performance versus conventional methods.

2. TIME VARYING CLUTTER MODEL

Doppler spectrum of surface backscatter from ocean nominally consists of two or more sharp Bragg lines at predicable frequencies. However, the Doppler spread of these lines indicates that the clutter return is, in fact, stationary only for a fraction of the coherent integration time (CIT) of the radar. Thus consider modeling the temporal clutter return at the receiver beamformer output as sum of modulated complex sinusoids. The temporal modulation sequence is assumed to be a non-stationary process with abrupt transitions in the modulation statistics. After beamforming, the clutter time series at the hypothesized range and azimuth cell is thus modeled as

$$c(n) = \sum_{k=1}^{r} \beta_k e^{j2\pi f_k n} h_k(n) \qquad (1)$$

for $n = [0, 2, ..., N-1]$, where the surface backscatter is assumed to consist of r Bragg lines with uncorrelated amplitudes β_k and nominal Doppler shifts given by f_k. The $N \times 1$ vector $h_k(n)$ is the Doppler spreading sequence

modulating the k^{th} Bragg line. To model non-stationary behavior, we assume that the modulation statistics change abruptly at certain time instants say $[n_1, n_2, ..., n_L]$ where L is the number of transitions. Furthermore, the modulation sequence $h_k(n)$ within each segment $0 \le n < n_2$, $n_1 \le n < n_2$ etc. is modeled as a band-limited stationary random process. Let $N_1, N_2, ...N_{L+1}$ denote the lengths of the $L+1$ segments of the modulation sequence. The temporal sequence modulating the entire CIT can be written as:

$$h_k(n) = \sum_{m=1}^{L+1} h_{km}(n - n_{m-1}) \quad (2)$$

where $h_{km}(n)$ is a stationary process that exists only for a short segment $0 < n < n_m$ and $n_0 = 0$. Here, we have assumed that the temporal sequences modulating different Bragg lines have identical non-stationary behavior although the individual sequences may be different. Furthermore, the modulation segments $h_{km}(n)$ are assumed to be uncorrelated with each other. Even though the sub-CIT sequences are band-limited, the overall modulation sequence $h_k(n)$ is not band-limited due to the presence of abrupt transition between the segments.

The radar return at the receiver contains strong non-stationary clutter, accompanied by a weak target return and background noise. The target return is assumed to be stationary across the full CIT. This is not unreasonable since a relatively unperturbed raypath is required to even detect high-speed aircraft targets from the background noise (which is usually lower than the clutter level). In vector notation, the *N x 1* beamformed time series snapshot, $\mathbf{x}$, for the range and azimuth under test can be expressed as

$$\mathbf{x} = \alpha \mathbf{s}(f_t) + \mathbf{c} + \mathbf{v} \quad (3)$$

where $\mathbf{s}(f_t)$ is the complex exponential of the target return with Doppler shift f_t and α is the unknown target amplitude. The vector $\mathbf{c}$ represents the temporally modulated clutter described in equation (1). The receiver noise component $\mathbf{v}$ is modeled as a zero-mean complex Gaussian vector with covariance $\sigma^2\mathbf{I}$. The objective here is to detect the presence of the target signal (i.e. $\alpha \neq 0$) in the presence of clutter and noise.

3. ATVAR PROCESSING

In this section, we first derive an expression for the Doppler spread clutter resulting from the model in equation (2) and then proceed to describe our clutter mitigation algorithm. In order to simplify the expression for the Doppler spread clutter, we make two assumptions, which have no impact on the performance of our algorithm. First, we assume that the sea clutter return consists of a single Bragg line with Doppler frequency f_1. We also assume that the modulation sequence $h_k(n)$ has only a single transition at some unknown location n_1. As the modulation sequence remains stationary in between the transitions, the modulation segments $h_{km}(n)$ can be expressed as sum of uncorrelated complex exponentials during this short period. If the full-CIT clutter $c(n)$ is partitioned into two segments $(L+1=2)$ at the transition point n_1, the sub-CIT clutter return can be expressed as

$$c_m(n) = \sum_{i=1}^{p} b_{mi} \exp(j2\pi(f_{mi} + f_1)n) \quad (4)$$

for $n_{m-1} \le n < n_m$ and $m = 1, 2$. Amplitudes b_{mi} of the modulated clutter frequencies $(f_{mi} + f_1)$ are uncorrelated within the segment as well as from one segment to another. Frequency resolution of the modulated clutter components is inversely proportional to the segment length N_m. Full-CIT Doppler processed clutter return at the receiver output is given by

$$C(f) = W(f) * \sum_{m=1}^{2} \sum_{i=1}^{p} \tilde{b}_{mi} \mathrm{sinc}(N_m \pi (f - (f_{mi} + f_1))) \quad (5)$$

where, $W(f)$ is the Fourier transform of the conventional Doppler processing window $w(n)$ and $\tilde{b}_{mi}$ is the product of clutter amplitude b_{mi} and the phase factors resulting from Fourier transforming operation. Doppler spread caused by non-stationary modulation of the clutter return affects the detection performance of the conventional processor in two ways. The wider sinc functions have broad temporal mainlobes $(\frac{1}{N_m} \gg \frac{1}{N})$, which can suppress weak targets that are close to the Bragg lines. Higher sidelobes caused by abrupt transitions lead to an increase in the overall sidelobe level thus masking weak targets that are even far away from the Bragg lines. To derive an expression for the sidelobe level, let us consider a Doppler frequency away from the clutter Bragg lines such that it is in the sidelobe of the sinc function. If the transition point is close to the middle of the CIT, the tapering window has negligible effect in combating the high sidelobes. In this case, the clutter sidelobe level is given by,

$$C(f_0) = \sum_{m=1}^{L+1} \sum_{i=1}^{p} E\{|b_{mi}|^2\} \mathrm{sinc}^2(N_m \pi f_0) \quad (6)$$

This equation also shows that the sidelobe levels increase with the number of transitions.

Our approach to clutter mitigation consists of designing an adaptive Doppler processor that suppresses the Doppler spread clutter while preserving the Doppler output of weak stationary targets. In this method, the full-CIT data is divided into shorter segments of length N_0 called 'sub-CITs' and the clutter return in each sub-CIT is modeled as an autoregressive process of relatively low order. Moreover, the number of sub-CIT's is assumed to be large compared to the number of abrupt transitions in the clutter data. Thus the AR model fails only for a relatively small number sub-CITs that encompass an abrupt transition. The full CIT clutter return $c(n)$ can be represented as a time-varying autoregressive (TVAR) process with abrupt change in the AR parameters from one sub-CIT to the next.

$$c(n) = -\sum_{k=1}^{M} a_k(n)c(n-k) + \varepsilon(n) \tag{7}$$

Here, M is the order of the TVAR process and $\varepsilon(n)$ is the non-stationary white noise process driving the TVAR all-pole filter. The time-varying AR parameters remain constant during the sub-CIT.

$$a_k(n) = a_{k,i} \qquad n = [(i-1)N_0, ..., iN_0 - 1] \tag{8}$$

The TVAR parameters in each sub-CIT are estimated using Burg AR algorithm by minimizing the sum of forward and backward prediction errors. The pole frequencies of the TVAR parameters represent the time-varying frequencies of the temporally modulated clutter given by equation (4). The TVAR parameters are used to extrapolate the sub-CIT data and compensate the Doppler resolution loss resulting from shorter correlation lengths N_m of the modulation function. The sub-CIT extrapolation is done using a data extrapolation method (DATEX) proposed by Swingler and Walker [3] in 1989. In this method, autoregressive linear prediction is used to extrapolate the data equally in both forward and backward directions. The full CIT data $x(n)$ is divided into sub-CIT segments $x_i(n)$ corresponding to $i = [1, 2, ..., N_s]$ and DATEX extrapolation is performed independently in each sub-CIT. Extrapolation of the i^{th} sub-CIT data is performed by IIR filtering the M endpoint data with the estimated AR parameters.

$$\begin{aligned} x_i(n) &= -\sum_{k=1}^{M} a_{k,i}^{*} x_i(n+k) \qquad -(N-N_0)/2 \le n < 0 \\ x_i(n) &= -\sum_{k=1}^{M} a_{k,i} x_i(n-k) \qquad N_0 \le n < (N-N_0)/2 \end{aligned} \tag{9}$$

The sub-CIT data is extrapolated to $(N - N_0)/2$ length in both forward and backward directions so that the extrapolated output spans the full CIT length. Conventional Fourier transform is performed on the extrapolated data $x_i(n)$ to obtain a high resolution Doppler spectrum.

$$X_{ei}(f) = X_{ei}(f) * W(f) \tag{10}$$

Here, $W(f)$ is the Fourier transform of the tapering window. Target returns in the sub-CIT data are not extrapolated by DATEX, as they are usually very weak compared to the clutter. The final step is to design a set of complex weights for combining the DATEX outputs of all sub-CITs coherently, so that the output SNR of a stationary target is maximized. For a hypothesized target Doppler frequency f_d, output SNR is maximized if the weights are chosen to be conjugate of starting phase of the target exponential $e^{j2\pi f_d n}$ in each sub-CIT. Coherently stitched ATVAR Doppler output can be expressed as:

$$X_e(f) = \sum_{i=1}^{N_s} e^{j\phi_i(f)} X_{ei}(f) \tag{11}$$

where, the phase factor is given by $\phi_i(f) = e^{-j2\pi f(i-1)N_0}$. At every hypothesized Doppler frequency f_d, the ATVAR output power $\left|X_e(f_d)\right|^2$ is compared to a preset threshold to detect the presence of targets. Successful ATVAR clutter mitigation requires that the number of bad sub-CIT's, which are corrupted due to their inclusion of abrupt transitions, be much smaller compared to the total number of sub-CITs.

4. RESULTS

Abruptly time-varying autoregressive (ATVAR) processing is applied to real over-the-horizon (OTH) radar data into which a stationary simulated target is injected. The radar uses a waveform with 5.2 Hz pulse repetition frequency and 25.4 seconds observation time (CIT). Detection performance of ATVAR method is analyzed by injecting a stationary target at 20 different range bins and 20 different Doppler bins in the sub-clutter region (-0.3 Hz to 0.3 Hz and 0.8 Hz to 1.2 Hz). TVAR model of order 6 and sub-CIT length 6.3 seconds (32 pulses) is used to detect the targets.

Figure 1 is a conventional range-Doppler map computed with non adaptive –96 dB sidelobe Taylor window. The injected target at range bin 36 is hardly seen due to strong Doppler spread clutter in between the Bragg lines. Figure 2 shows the range-Doppler map computed using ATVAR processing. Strong target peak can be clearly seen in the plot. Furthermore, Bragg lines are sharper and the sub-clutter visibility is significantly improved. The target-to-clutter gain achieved by ATVAR processing can be observed more precisely in the Doppler cuts shown in Figure 3. ATVAR provides more than 5 dB gain in target signal to clutter plus noise ratio (SCNR) while the conventional Doppler spectrum overshadows the target with Doppler spread clutter. The last plot, figure 4, shows the detection probability of the two methods as a function of injected target SNR for a fixed false alarm probability of 0.1. A constant false alarm rate (CFAR) detector is

implemented by normalizing the target power with respect to the background clutter level.

5. CONCLUSIONS

A partially adaptive Doppler processing technique aimed at mitigating non-stationary clutter for improved target detection has been proposed. This method models the clutter return using an abruptly time-varying AR model to exploit the non-stationarity. ATVAR processing improves the target detection by mitigating the effects of abrupt changes in the temporal modulation function while preserving the target gain against white noise.

ACKNOWLEDGEMENT

This work was supported by ONR Code 313 and by the Naval Research Laboratory, Washington, DC.

REFERENCES

[1] J. Parent, and A. Bourdillon, "A method to correct HF sky wave backscattered signals for ionospheric frequency modulation," *IEEE Transactions on Antennas and Propagation*, Vol. 36, pp. 127-135, 1988.

[2] K. Harmanci, and J. Krolik, "Matched window processing for mitigating over the horizon radar spread Doppler clutter," *Proceedings of the ICASSP 99 conference*, Vol. 5, May 1999.

[3] D. Swingler, and R. Walker, "Line-Array Beamforming using Linear Prediction for Aperture Interpolation and Extrapolation," *IEEE Transactions on Acoustics*, Vol. 37, No.1, pp. 16-30, 1989.

[4] Y. Abramovich, N. Spencer, and M. Turley, "Adaptive Time-Varying Processing for Stationary Target Detection in Nonstationary Interference," *Adaptive Sensor and Array Processing,* MIT Lincoln Laboratories, 2005.

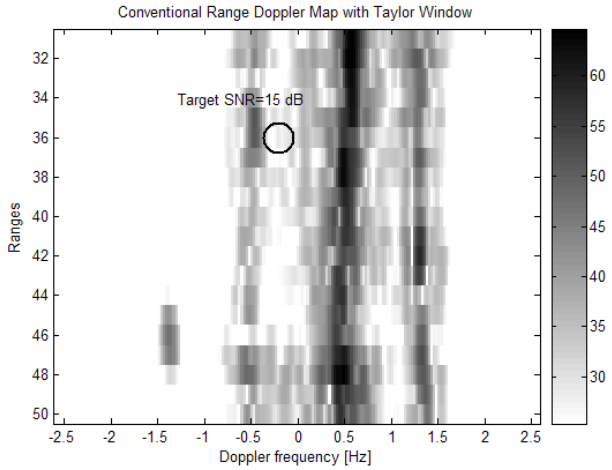

Figure 1: Range-Doppler Plot with Conventional Processing

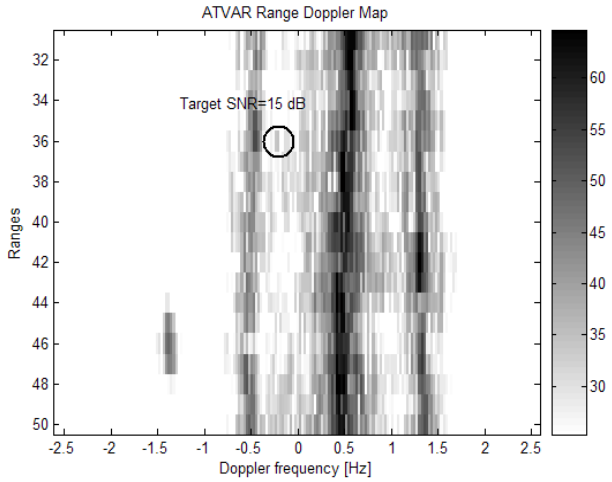

Figure 2: Range-Doppler Plot with ATVAR Processing

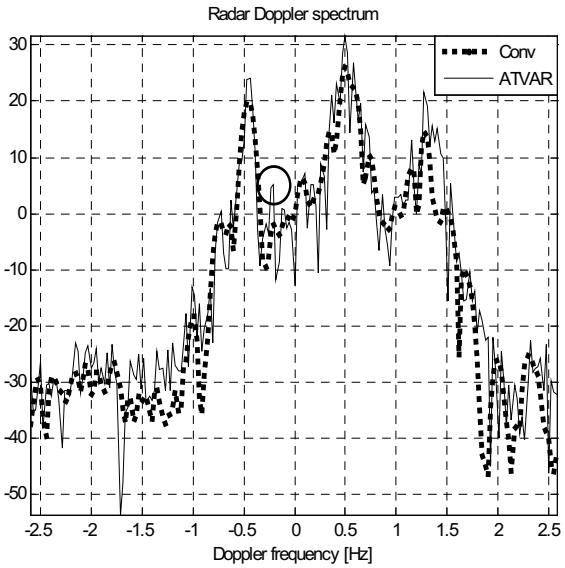

Figure 3: Comparison of Conventional and ATVAR spectrum.

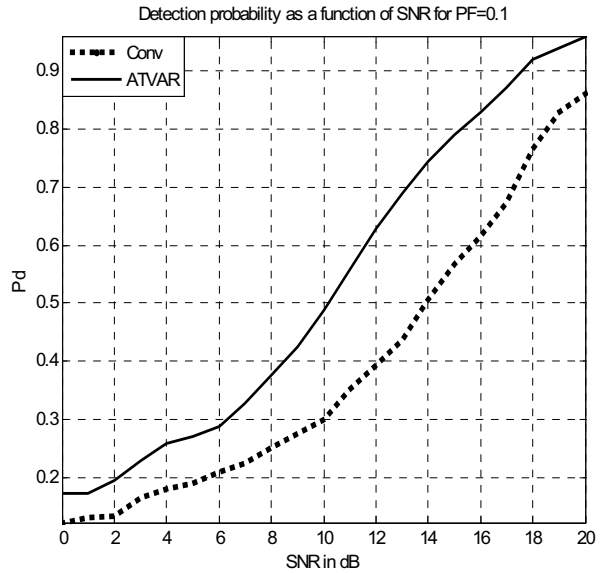

Figure 4: Detection Performance as a function of SNR